

## Neutron-diffraction studies on the time dependence of the oxygen ordering in $\text{La}_2\text{NiO}_{4.105}$

J. E. Lorenzo\* and J. M. Tranquada

*Department of Physics, Brookhaven National Laboratory, Upton, New York 11973*

D. J. Buttrey and V. Sachan

*Department of Chemical Engineering, University of Delaware, Newark, Delaware 19716*

(Received 18 May 1994; revised manuscript received 13 September 1994)

We present a single-crystal neutron-diffraction study of the time dependence of the interstitial oxygen ordering in  $\text{La}_2\text{NiO}_{4.105}$ . We have studied the kinetics of the growth of the intercalated *Bmab* phase at different temperatures below the phase transition temperature ( $\approx 290.5$  K). The transformation appears to occur by homogeneous nucleation and growth. The time dependence of the transformed fraction follows a universal curve when the time variable is scaled appropriately. The transformation rate peaks near 265 K. The domain size measured after saturation decreases with decreasing quench temperature due to the increase in nucleation rate.

We have shown recently<sup>1-3</sup> that the nonstoichiometric compound  $\text{La}_2\text{NiO}_{4+\delta}$  has a very rich oxygen-content phase diagram. The incorporation of extra oxygen into the lattice is favored by distortions involving tilts of the  $\text{NiO}_6$  octahedra about a [110] axis of the high-temperature tetragonal unit cell, similar to those that occur in the low-temperature orthorhombic phase (space group *Bmab*) for  $\delta = 0.00$ . Individual added oxygens will tend to sit between adjacent LaO layers at positions  $(\frac{1}{4}, \frac{1}{4}, \frac{1}{4})$  of the *Bmab* structure.<sup>4</sup> However, an interstitial oxygen will repel its four oxygen nearest neighbors, causing the associated octahedra to tilt away from it and disrupting the local tilt pattern.

In the oxygen-excess range  $0.058 \leq \delta < 0.11$  we have found evidence that the interstitials tend to cluster in layers that are spaced periodically along the *c* axis.<sup>2</sup> The spatial ordering of interstitial oxygens brings about the appearance of superlattice peaks of the type  $(0, k, l \pm \Delta)$  with *k* odd and *l* even,<sup>2,3</sup> the intensity for which comes from the tilt pattern of the octahedra rather than from the interstitial oxygens themselves. The structure between interstitial layers has the *Bmab*-type tilt pattern, i.e., with the tetragonal [110] direction as tilt axis. The interstitial layers induce antiphase domain boundaries, resulting in the displaced superlattice peaks.

The ordering of the interstitial layers is quite similar to the staging of alkali atoms intercalated in graphite, and the diffraction pattern can be well described using the formulas for random ordering in a layer-type lattice.<sup>5,6</sup> Borrowing the concept of staging, the stage order is defined as the number of Ni-O planes separating interstitial oxygen layers. Well-defined stage-2 and stage-3 phases appear to exist, with phase separation at intermediate oxygen concentrations. Despite the apparent immiscibility of different stages, intergrowth-type defects (or stacking faults) tend to occur within an individual phase.

In the present work we study the time dependence of the oxygen ordering in a sample with  $\delta = 0.105$ .  $\text{La}_2\text{NiO}_{4.105}$  undergoes a sluggish phase transition at

290 K from disordered tetragonal to a phase with stage-2 ordering.<sup>2,3</sup> When cooled slowly through the transition, superlattice reflections appear at positions  $(0, k, l \pm (\frac{1}{2} - \epsilon))$  with *k* odd and *l* even. For perfect stage-2 order, one would expect  $\epsilon = 0$ ; however we find  $\epsilon \geq 0.015$ , due to the presence of stacking faults. The observed peak positions and widths are well described by a model that includes a small fraction of randomly positioned stage-3 defects.<sup>2</sup> The degree of stacking order is quite sensitive to the cooling rate, such that rapid cooling results in a high concentration of stacking faults.

The experiment was performed on the double-monochromator, triple-axis spectrometer H9 located on the cold neutron source at Brookhaven's High Flux Beam Reactor. Measurements were taken at 5 meV incident energy, with a beryllium filter before the monochromator to remove high-order neutrons. Collimation was 60'-40'-30'-s-40'-40' (corresponding to an effective collimation in the normal four-collimator configuration of 20'-40'-s-40'-40'), as seen from reactor to detector. The sample was the same one used in previous experiments.<sup>2,3</sup>

The experimental procedure consisted of "quenching" the sample from 310 K to the selected quench temperature,  $T_q$ , below  $T_c = 290.5$  K, and monitoring the peak intensity of the  $(0, 1, 4 + \frac{1}{2} - \epsilon)$  superlattice reflection as a function of time. Several runs were also performed on samples quenched from 300 K, which indicate no dependence on the choice of the starting temperature. The sample was cooled in a Displex refrigerator at a rate of 3 K/min, and starting time was measured from the point at which the sample temperature reached the selected value. In Fig. 1 we present the peak intensity versus time results for all measured temperatures. Only at 290 K (indicated by dots) was the transformation sufficiently slow to allow a full peak scan at each sampling point.

Before discussing the time dependence, we first consider the results of *Q* scans performed along the *k* and *l* directions in the  $t \rightarrow \infty$  limit, i.e., after the peak intensity has saturated, as a function of the quench temperature.

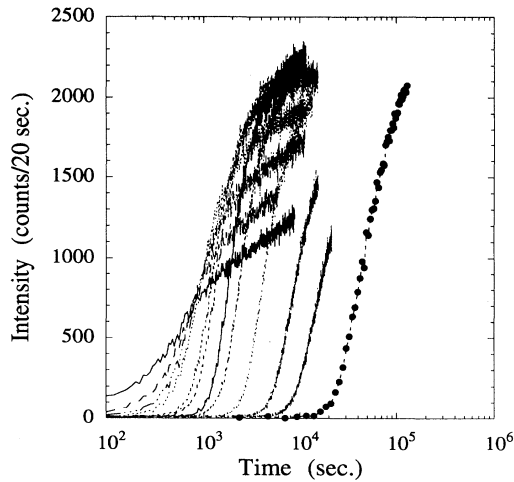


FIG. 1. Peak intensity as a function of time for different quenching temperatures. From left to right the temperatures are 255 K, 260 K, 265 K, 270 K, 275 K, 277.5 K, 280 K, 282.5 K, 285 K, 287.5 K, 288.7 K, and 290 K (dots).

Note that the degree of intensity saturation achieved is somewhat obscured by the logarithmic time scale used in Fig. 1. For temperatures below 285 K, we have typically measured to 10 times the characteristic time scale, which will be defined below. At higher temperatures it was not practical to wait for the same number of characteristic units because of the very slow kinetics. Typical peak profiles can be found in Ref. 2.

As shown in Fig. 2(a), the peak position along  $l$  tends to decrease as a function of  $T_c - T_q$ . This decrease correlates with an increase in the resolution-corrected peak width, shown in Fig. 2(b), which is found to be surprisingly isotropic. (Above 280 K the peak widths along  $k$  and  $l$  are resolution limited.) The peak width is inversely proportional to the domain size. The dependence of domain size on  $T_q$  can be explained as follows. The nucleation rate depends on the difference in free energies between the ordered and disordered states, which increases with  $T_c - T_q$ . However, when more domains are nucleated the average domain size must decrease. Once the transformation is complete the initial domain distribution might be expected to further coarsen by the accretion of smaller domains into larger ones. Such a coalescence is presumably inhibited by substantial energy barriers associated with domain walls between the four distinct structural domain types: two due to orthorhombic twinning, and two more due to the degeneracy in the location of the interstitial layers in the lattice. Along the  $c$  axis, domain boundaries will be similar to stacking faults, thus causing a shift in the peak position.

The peak intensity, displayed in Fig. 2(c), exhibits a linear decrease below 280 K. On the other hand, the integrated intensity, which we expect to be proportional to the transformed volume fraction, exhibits a more gradual variation with the quench temperature, as shown in Fig. 2(d). The decrease in intensity on approaching  $T_c$

reflects the decrease in the long-range order commonly observed near order-disorder transitions. The falloff below 260 K indicates incomplete ordering due to kinetic limitations.

We now turn to the analysis of the time dependence

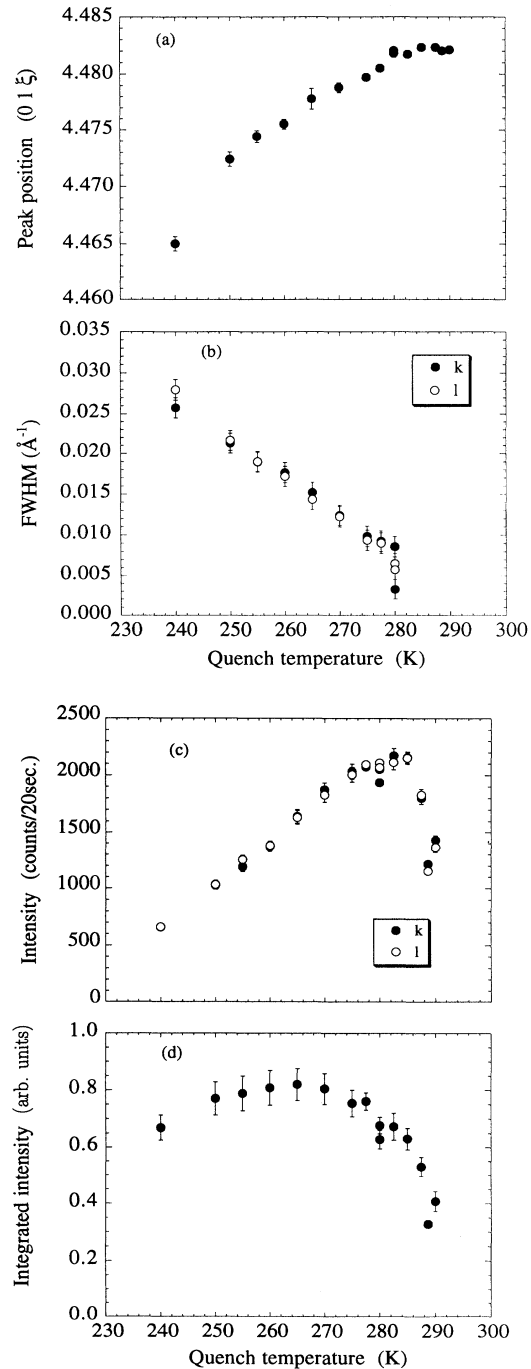


FIG. 2. Peak position along the  $l$  direction (a), FWHM (b), peak intensity (c), and integrated intensity (d) as a function of the quenching temperature. Full circles and open circles in (b) and (c) correspond, respectively, to scans along  $k$  and  $l$  directions.

of the ordering. Ideally, one would like to measure the full  $Q$  dependence of the superlattice peak as a function of time. However, because of the weak scattering rate and the need for reasonable time resolution, the time dependence was probed through measurements of the peak intensity, which we assume to be proportional to the integrated intensity. This proportionality depends on the FWHM and weakly on time. Significant variations in the peak width with time would invalidate this assumption. To the extent that we have checked, the observed width changes, which are limited by the spectrometer resolution, are small. At 290 K, where the transformation rate is low enough to allow full scans at each time step, the peak width is resolution limited at all times. For  $T = 270$  K at the half-of-saturation point, the widths of  $k(l)$  scans are 10% (18%) larger than at saturation. We will ignore such variations in the following analysis. The point at which the intensity was monitored at each quench temperature was adjusted so as to correspond to the approximate peak position observed at long times.

Under the assumption that, at a given temperature, the peak intensity,  $I(t)$ , is directly proportional to the integrated intensity, we can define the relative transformed volume fraction,  $Y(t)$ , as

$$Y(t) = \frac{I(t) - I(0)}{I(t \rightarrow \infty) - I(0)}. \quad (1)$$

The data for  $T \geq 275$  K in Fig. 1 can then be scaled onto a universal curve (Fig. 3) by plotting  $Y(t)$  versus  $\tau = t/t_{1/2}$ , where the characteristic time  $t_{1/2}$  is defined by  $Y(t_{1/2}) = 0.5$ . (For  $T > 285$  K, the data were normalized so as to fall on the curve, since the measurements did not approach sufficiently close to saturation.) As we decrease the quenching temperature below 275 K the sam-

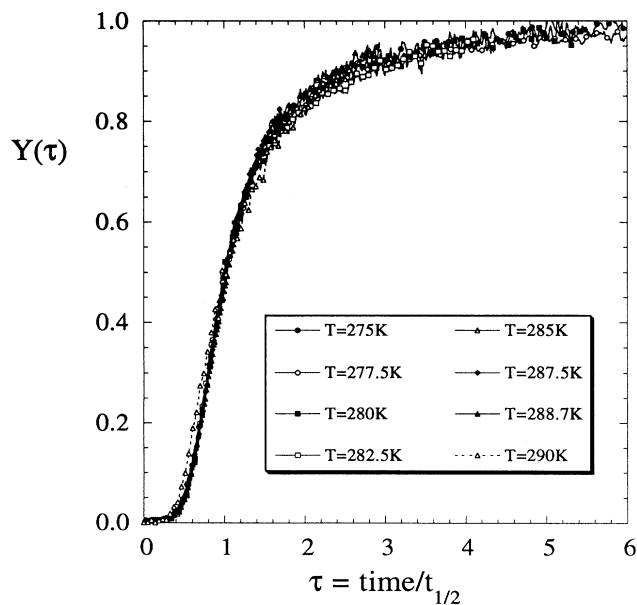


FIG. 3. Demonstration of scaling for data measured at and above 275 K.  $t_{1/2}$  is defined as the time at which the transformation has gone to half completion.

ple starts to order before reaching the selected quenching temperature. The normalized plot of the peak intensities shows a substantial departure from the universal curve for these temperatures. However we find that these data can be made to fall onto the universal curve by adjusting the initial time. This redefinition corresponds to the situation where the growth process starts from clusters formed during the time the sample takes to go from  $T_c$  to the selected quenching temperature. Note that there are no physical reasons to suppose that below 275 K the growth mechanism may be different from that observed above 275 K.

The ordering of the intercalated oxygen appears to occur by the mechanism of homogeneous nucleation and growth. A simple model for the kinetics of such a transformation was worked out by Kolmogorov, Johnson, Mehl, and Avrami (KJMA).<sup>7</sup> It has been successfully applied to the order-disorder transformation in  $\text{Cu}_3\text{Au}$  (Refs. 8 and 9) and the  $\text{NaCl-CsCl}$  transformation in  $\text{RbI}$  under pressure.<sup>10,11</sup> This model is completely specified by two time-independent parameters: the rate of nucleation,  $\Gamma_0$ , and the linear velocity, assumed to be isotropic, at which the nuclei grow after nucleation,  $v$ . The expression for the transformed volume fraction is of the form

$$Y(t) = 1 - e^{-D\tau^{d+1}}, \quad (2)$$

where  $D$  is a dimensionless constant that depends on the dimensionality,  $d$ , of the nucleation and growth process, and

$$t_{1/2} = \left( \frac{\alpha}{\Gamma_0 v^3} \right)^{1/(d+1)}, \quad (3)$$

with  $\alpha$  a numerical constant. Analysis of the data in Fig. 3 reveals that, in the present case,  $Y(t)$  varies as  $t^4$  up to  $0.7t_{1/2}$ , indicating that  $d = 3$ , and hence  $D = \ln 2$  and  $\alpha = 4$ . The result of this model is shown in Fig. 4 by the dashed line labeled  $Y_0$ . Unfortunately, the final stages of growth for our sample are not well described by this simple model. The agreement is not improved by changing the effective dimensionality  $d$ .

To describe our data using the KJMA equation, it would be necessary to replace the simple  $t^4$  factor in the exponent with a function that crosses over to a weaker  $t$  dependence at large  $t$ . A similar crossover behavior has been observed in a study of ordering in diblock copolymers by Harkless *et al.*<sup>12</sup> In that system the transformation never reached 100%. The same is also true in the case of  $\text{La}_2\text{NiO}_{4.105}$ . As discussed in Ref. 2, a small amount of the disordered tetragonal phase always survived in the low-temperature ordered orthorhombic phase, even when the sample was cooled very slowly. Doman and Nagler<sup>13</sup> developed a model for such a transformation into a two-phase coexistence region in which the free-energy difference between ordered and disordered phases decreases as the transformation progresses. While they obtained a useful formula, it does not explicitly contain the scaling behavior that we have observed.

To develop a phenomenological formula that both reproduces our experimental data and exhibits scaling, we

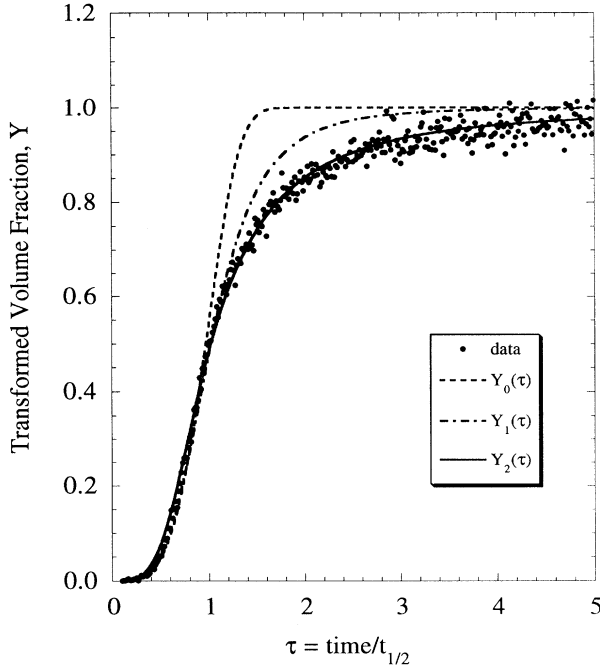


FIG. 4. Fitting of the transformed volume fraction to the three expressions derived in the text. Data correspond to a quenching temperature of 275 K.

start with a simple derivation of the KJMA equation. The rate of change of transformed volume fraction  $Y$  will depend on the nucleation rate and the rate of growth of the orthorhombic domains. We assume that the nucleation rate per unit volume of the tetragonal phase is a constant  $\Gamma_0$ , at a given temperature. However, the relative fraction of the tetragonal phase decreases with time, giving the net nucleation rate,  $\Gamma$ , an effective time dependence,

$$\Gamma(t) = \Gamma_0[1 - Y(t)]. \quad (4)$$

If we suppose that the domains of the orthorhombic phase grow isotropically in three dimensions, with a velocity  $v$ , then the rate of growth of the volume fraction of the orthorhombic phase is given by

$$\frac{dY}{dt} = \Gamma_0 v^3 t^3 (1 - Y). \quad (5)$$

The solution of this differential equation is the KJMA equation for  $d = 3$ . If the transformation is not to go to completion, both the nucleation and growth rates must be reduced at late times. We take account of this reduction in a phenomenological way by including an extra factor of  $[1 - Y(t)]^n$  on the right-hand side of Eq. (5), where  $n$  is to be determined by comparison with experiment. Note that we must also change the meaning of  $Y$  from absolute volume fraction to volume fraction relative to the transformed volume at saturation. We then obtain the equation

$$\frac{dY_n}{d\tau} = \alpha \tau^3 (1 - Y_n)^{n+1}, \quad (6)$$

where we have introduced the scaled time  $\tau = t/t_{1/2}$  with  $t_{1/2}$  defined by Eq. (3). If  $n$  is an integer, then the differential equation is easily solved. For  $n = 1$  we find

$$Y_1(\tau) = \frac{\tau^4}{1 + \tau^4}, \quad (7)$$

with  $\alpha = 4$ . For  $n = 2$  one obtains

$$Y_2(\tau) = 1 - \frac{1}{\sqrt{1 + 3\tau^4}}, \quad (8)$$

with  $\alpha = 6$ . In Fig. 4 we have plotted the results for these three different models. Whereas the first two models predict a faster approach to saturation, the third one reproduces fairly well the observed experimental behavior at all times. It effectively describes both the crossover and scaling behaviors.

The temperature variation of  $t_{1/2}^{-1}$ , shown in Fig. 5, appears to vary as  $(T_c - T_q)$  close to  $T_c$ . The ordering temperature obtained by extrapolation is 290.5 K. At around 265 K,  $t_{1/2}^{-1}$  goes through a maximum, decreasing at lower temperatures, as expected for this kind of process.<sup>14</sup> This behavior is the result of a competition between the nucleation rate, which increases rapidly below  $T_c$ , and the domain wall velocity, which is limited by the oxygen diffusion rate and which decreases rapidly with falling temperature.

In conclusion, we have studied the kinetics of the oxygen ordering in  $\text{La}_2\text{NiO}_{4.105}$  as a function of the quenching temperature. The interstitials develop stage-2 order below a transition temperature of 290.5 K. Stacking defects are observed, with the number of these defects increasing with the “depth” of the quenching. We have also shown that the kinetics of the oxygen ordering at all measured temperatures can be well understood through the nucleation and growth mechanism. The initial stage

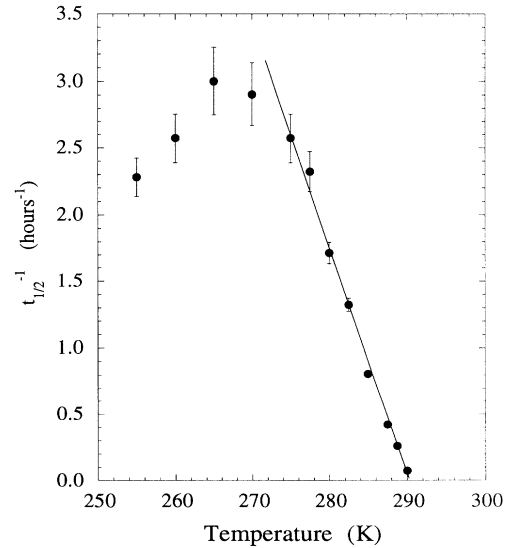


FIG. 5. Temperature variation of  $t_{1/2}$ . The straight line corresponds to  $t_{1/2}^{-1} = 0.16(T_c - T)$ , with  $T_c = 290.5$  K.

of the ordering is characterized by a  $t^4$  time dependence, while the approach to saturation occurs more slowly than that predicted by the KJMA model with  $d = 3$ .<sup>7</sup> We have developed a phenomenological model to account for this behavior, involving a self-consistent reduction in the growth and nucleation rates at late stages, that describes the experimental data reasonably well.

We gratefully acknowledge helpful discussions with J. D. Axe and S.E. Nagler. Work at Brookhaven National Laboratory was carried out under Contract No. DE-AC02-76CH00016, Division of Materials Sciences, U.S. Department of Energy. D.J.B. and V.S. acknowledge support from the National Science Foundation under Contract No. DMR-8914080.

---

\* Present address: European Synchrotron Radiation Facility, B.P. 220, F-38043 Grenoble Cedex, France.

<sup>1</sup> D. E. Rice and D. J. Buttrey, *J. Solid State Chem.* **105**, 197 (1993).

<sup>2</sup> J. M. Tranquada, Y. Kong, J. E. Lorenzo, D. J. Buttrey, D. E. Rice, and V. Sachan, *Phys. Rev. B* **50**, 6340 (1994).

<sup>3</sup> J. M. Tranquada, D. J. Buttrey, and D. E. Rice, *Phys. Rev. Lett.* **70**, 445 (1993)

<sup>4</sup> J. D. Jorgensen, B. Dabrowski, S. Pei, D. R. Richards, and D. G. Hinks, *Phys. Rev. B* **40**, 2187 (1989).

<sup>5</sup> S. Hendricks and E. Teller, *J. Chem. Phys.* **10**, 147 (1942).

<sup>6</sup> C. D. Fuerst, J. E. Fischer, J. D. Axe, J. B. Hastings, and D. B. McWhan, *Phys. Rev. Lett.* **50**, 357 (1983).

<sup>7</sup> A. N. Kolmogorov, *Bull. Acad. Sci. (USSR)* **3**, 355 (1947); W. A. Johnson and R. F. Mehl, *Trans. Am. Min. Metal. Eng.* **135**, 416 (1939); M. Avrami, *J. Chem. Phys.* **7**, 1103

(1939); **8**, 212 (1940); **9**, 177 (1941).

<sup>8</sup> S. Nishihara, Y. Noda, and Y. Yamada, *Solid State Commun.* **44**, 1487 (1982).

<sup>9</sup> S. E. Nagler, R. F. Shannon, Jr., C. R. Harkless, M. A. Singh, and R. M. Nicklow, *Phys. Rev. Lett.* **61**, 718 (1988).

<sup>10</sup> N. Hamaya, Y. Yamada, J. D. Axe, D. P. Belanger, and S. M. Shapiro, *Phys. Rev. B* **33**, 7770 (1986).

<sup>11</sup> J. D. Axe, *Jpn. J. Appl. Phys.* **24**, 46 (1985).

<sup>12</sup> C. R. Harkless, M. A. Singh, S. E. Nagler, G. B. Stephenson, and J. L. Jordan-Sweet, *Phys. Rev. Lett.* **64**, 2285 (1990).

<sup>13</sup> E. Domany and S. E. Nagler, *Physica A* **177**, 301 (1991).

<sup>14</sup> D. A. Porter and K. E. Easterling, *Phase Transformations in Metals and Alloys* (Van Nostrand Reinhold, Wokingham, Berkshire, England, 1981), Chap. 5, pp. 263–290.